Egyptian Journal of Chemistry

http://ejchem.journals.ekb.eg/

Low Cost Agro-Residue Derived Biosorbents: Synthesis, Characterization and Application for Removal of Lead Ions ffrom Aqueous Solutions

Asmaa Abdou Serage, Mohsen M Mostafa and Magda A Akl*

Chemistry *Department*, Faculty of Science, Mansoura University, Mansoura 35516, Egypt

Abstract

In the present study three biosorbents are prepared from orange peel bio-wastes. These are the raw orange peel (RR), the sodium hydroxide modified orange peel (RN) and the sulfuric acid modified orange peel (RS). The prepared biosorbents are characterized by scanning electron microscopy (SEM), Fourier transform infrared spectroscopy (FT-IR), point of zero charge. Batch adsorption method is applied to determine the optimum operational parameters for lead ion removal from aqueous solutions such as pH, initial concentration of metal ion, contact time and adsorbent dosage. Kinetic models have been applied to test the experimental data to determine the mechanism of adsorption and its potential rate-controlling step. The obtained kinetics data revealed that the adsorption process of lead ion is more fitted to pseudo-second order than pseudo-first order. Equilibrium data showed that adsorption of lead ions fitted well with Langmuir equilibrium isotherm model. Thermodynamic parameters ΔG°, ΔH° and ΔS° parameters have been investigated. The negative values of ΔG° of all biosorbents explain the spontaneous behavior of adsorption process. The negative values of ΔH° can explain the exothermic behavior of (RR, RN), while positive value of ΔH° can explain the endothermic behavior of (RS). The prepared orange peel derived biosorbents were successfully applied for removal of lead ion from different water samples.
Keywords: biosorbents, lead(II), orange peel, adsorption

1. Introduction

Pollution of natural water resources by heavy-metal ions is one of the most important problems that faces and threats the whole of the word.

These contaminants are produced from liquid wastes discharged from a number of industries such as electroplating, dyes and dye intermediates, textiles, tanneries, oil refineries, electroplating, mining, smelters, etc [1-3]. Heavy metal toxicity can result in serious danger to humans such as having cancer[4], because they are not biodegradable into harmless end products [5]. So, governments have enacted laws to hinder the of discharging heavy metals into water bodies or using toxic substances such as lead[6]. Lead is considered as one of the most toxic heavy metals. It is listed as the second most hazardous substance by The Agency for Toxic Substances and Disease Registry (The ATSDR 2011)[7] .

Lead contamination in the environment usually comes from wastewaters or effluents from lead mining, battery recycling, electronics assembly plants, and military facilities, as well landfill leachate and urban rainwater runoff[8]. It has a moderately low solubility and will precipitate as a solid in moderate to high reducing systems [9].

The presence of lead ions in drinking water is known to cause various types of serious health problems as anemia, brain damage, mental deficiency, dysfunction of kidneys, liver, and central nervous system in humans, especially in children and behavioral problems in humans leading to death in extreme cases [10]. Chronic exposure to lead may result in birth defects, mental retardation, autism, psychosis, allergies, dyslexia, hyperactivity, weight loss, shaky hands, muscular weakness, and paralysis (beginning in the forearms). The permissible limit of lead ion in drinking water is 0.05 mg /L according to the US Environmental Protection Agency (EPA) [11].

*Corresponding author e-mail: magdaakl@yahoo.com.; (Magda Akl).
Receive Date: 22 February 2022, **Revise Date:** 09 March 2022, **Accept Date:** 24 April 2022, **First Publish Date:** 24 April 2022
DOI: 10.21608/EJCHEM.2022.123416.5516

Several techniques were exercised for heavy metals removal from wastewater like adsorption, sedimentation and flocculation[12-18], chemical precipitation[19], ion exchange[20-22], membrane separation methods[23], photo-catalysis, and solvent extraction[24].

Of these applicable processes, adsorption has gained considerable attention due to its low cost, ease of the bio-waste materials availability, easy operation, reuse and regeneration abilities, higher removal capacity over a wide range of pH and ability to remove the complex form of metals[25-27].

Agriculture bio-wastes in the form of peels of certain vegetables, fruits and the leaves shredded from various plants and trees are widely used in the recent years as an excellent source for removal of different pollutants from water resources. Therefore, the relevant utilization of these bio-wastes should be the priority in order to keep the environment clean and green. Bio-adsorption is one such innovative technology where a simple or chemically modified adsorbent can be developed from certain available plant materials like husks, leaves, peels, stems, branches, and pods. Extensive efforts are being made in this field with the aim of preparing low cost bio-waste-based novel adsorbents for the efficient removal of heavy metals from wastewater[28-32].

The by-product orange peel residue is one of the valuable biomass wastes. The use of orange peel as an adsorbent material presents strong potential due to its high content of cellulose, pectin (galacturonic acid), hemicellulose and lignin. These components bear various polar functional groups including carboxylic and phenolic acid groups to be involved in metal binding and are biopolymers admittedly associated to the removal of heavy metals[27, 33-38].

The aim of the present study is to prepare low cost bio-waste-based adsorbents from the orange peels by product and thoroughly studying their efficiency for the removal of lead ion from water samples.

2. 2. Materials and methods.

2.1. Reagents and solutions.

Lead nitrate as a source of the metal under studying and all other chemicals that are used in our work are analytical grade and purchased from Sigma-Aldrich. 1000 (ppm) stock solution of Pb (II) is prepared by dissolving Pb $(NO_3)_2$ in de-ionised water and acidified with few drops of concentrated HNO_3 to prevent any possible hydrolysis. Batch adsorption experiments are performed after preparation of different working diluted solutions from 1000(ppm) bulk stock solutions.

2.2. Instrumentation.

UV-Vis spectrophotometer (Chrom Tech-Co., Ltd., USA) is used for spectrophotometric determination of Pb (II) at λ_{max}= 520 nm using 4-(2-Pyridylazo) Resorcinol monosodium salt (PAR). pH meter (Hi 931401, HANNA, Portugal) was used to measure the pH of all the prepared solutions.

2.3. Preparation of orange peel derived bio-sorbents.

2.3.1. Preparation of raw orange peel (RR).

The orange peel (OP) residues were collected, dried in sunlight and then cut into small pieces. After that, they were washed with about 5% solution of concentrated HCl several times in order to remove all dirty objects and any of outstanding objects. After washing with HCl solution they were washed with de-ionized water several times until the pH of water supernatant is HCl free (neutral pH). The Prepared precursors were dried in an oven at (105-110) ºC, overnight (or till completely drying).

2.3.2. Preparation of sodium hydroxide (NaOH) modified orange peel (RN).

To prepare the RN, raw orange peel (RR) was soaked in about 1L of NaOH solution (0.5 M) for 24hrs and occasionally stirred. After repeated decantation and filtration, the modified biomass (RN) was washed with double distilled water until the solutions reached a pH value of 7.0, and then dried in an oven at (105-110) ºC till completely drying. Here the sample is ready to be used.

2.3.3. Preparation of sulfuric acid activated orange peel (RS).

The prepared RR was carbonized firstly at (450-550) ºC in stainless steel reactor in absence of air to prepare the orange peel char (RC). After that, carbonized char (RC) is refluxing with concentrated sulfuric acid by ratio (RC: H_2SO_4 equal 1:10 W/V) for about 6hrs was done. This mixture was cooled followed by soaking in double distilled water several times for washing to from any un-reacted acid till the solutions reached a pH value of 7.0. After repeated decantation and filtration, the activated carbon sample (RS) was dried in an oven at (105-110) ºC till completely drying.

2.4. Characterizations

2.4.1. Fourier Transform infrared spectroscopy (FT-IR).

FT-IR spectra of the prepared bio-sorbents were collected using KBr-pressed discs using a Shimadzu 5800 Fourier FT-IR transform spectrometer. Jasco instrument (Model 6100, Japan); where, the obtained data was recorded between 4000 and 400 cm^{-1}.

2.4.2. BET Surface area.

The N_2 adsorption–desorption isotherm was used to determine surface area using the Brunauer–Emmett–Teller (BET) equation.

2.4.3. Scanning electron microscopy (SEM).

Scanning electron microscopy images were taken by using JSE - T20 (JEOL, Japan) microscope having an acceleration voltage of 40 kV.

2.4.4. Energy Dispersive X-ray spectroscopy (EDX).

EDX of the samples was measured using a (JSM-6510LV) *instrument*.

2.4.5. Surface pH, point of zero charge.

Analysis of the point of zero charge pH (pH_{PZC}) was determined using the pH drift method [39] .

2.5. Batch adsorption.

Batch adsorption was carried out in 100 ml flasks. Typically, an aqueous solution of Pb $(NO_3)_2$ was prepared at the initial Pb (II) concentration of 50 mg/L. 0.05 g of untreated or chemically-treated orange peels bio-sorbents was added into the flasks. Then, the pH of each solution was adjusted to 5.0 with (0.1 mol L^{-1} HCl and 0.1 mol L^{-1} NaOH) except for the influence of pH studies in which the pH ranged between (1 and 7).

The mixture was then shaken at a shaking rate of 150 rpm for 2 hours using a thermostatic shaker at the temperature of 25 °C. The adsorbents were separated and the remaining metal ion in aqueous solution was measured spectrophotometrically at λ_{max}=520 using PAR.

The sorption capacity ($mg.g^{-1}$) and recovery % of Pb (II) by the adsorbents was calculated using equations 1 and 2, respectively.

$$q_e = \frac{(C_o - C_e)V}{W} \quad (1)$$

$$\%R = \frac{(C_o - C_e)}{C_o} \times 100 \quad (2)$$

Where, C_o and C_e are the initial and equilibrium concentration of Pb (II) solutions in (mg/g), respectively. V is the volume of the mentioned adsorbates solution (L) and W is the mass of the adsorbents (gm).

Where, %R is the removal percentage of adsorbates from aqueous solution.

For sorption isotherm, metal ion concentrations in the range of 25-750 mg L^{-1} were examined at 25°C with pH 5 for 2 h. To study thermodynamic parameters, different metal ion concentrations were chosen at pH 5 with different temperatures between 25-60 °C.

For adsorption kinetics and isotherm studies, initial Pb (II) concentrations were varied between 50 and 300 mg/L. The experiments were conducted in a similar way as described above using the obtained data to determine the proposed kinetic models (pseudo-first order, pseudo-second order, Intraparticle diffusion, and Boyed model on activated sample.

For the adsorption isotherm validation, the data at the equilibrium was used to study Langmuir and Freundlich, isotherm models.

3. 3. Desorption study.

In order to study reusability of the prepared bio-sorbents, desorption study was performed. Firstly, adsorption of the studied adsorbate was done. Then, the RR and RN samples were washed gently with water to remove any of unsorbed materials. The samples were dried in an oven at (105-110) ºC. Known weight of the loaded carbon (0.05 gm) was shaken with different concentrations of HCl ranging from (0.1-0.4) M. The solutions were filtered and the % of desorption of metal ions from adsorbents was calculated.

De-sorption%

$$= \frac{amount\ dseorbed\ to\ thesolution\ (mg/l)}{amount\ adsorbed\ on\ activated\ sample\ (mg/l)} \times 100 \quad (3)$$

3. Results and discussion.

3.1. Surface characterization

3.1.1. FTIR

The FTIR analysis of RR, RN, and RS bio-sorbents before and after adsorption of Pb (II) was carried out to predict the role of surface groups on Pb (II) adsorption. The FTIR spectrum was shown in Figure (1, a-c).

- In all samples the broad and intense absorption peaks at (3427-3440) cm^{-1} correspond to the O-H stretching vibration of cellulose, pectin, absorbed water, hemicellulose, and lignin. Also we can observe that all samples have shoulders observed in the region between (2925-2852) cm^{-1} which are

a result of asymmetric and symmetric vibrations of methylene group(C-H)[40] .

- In case of RR sample before and after lead adsorption (Fig.1, a), the peaks at (1633-1629) cm^{-1} due to presence of C=O stretching vibration. The small shift of this bands may give an indication to decrease the concentration of the C=O group which may be the point at which the metal bind the sample surface.
- After modification of RR with sodium hydroxide new beaks appear.
  - There is new beak that appeared at (1624) cm^{-1} in case of RN, which is attributed to C=O stretching vibration.
  - The peak at (1427) cm^{-1} in case of RN sample corresponds to (C=C) in aromatic rings.
  - In case of RN sample, the band appears at (2146) cm^{-1} is due to vibration of(C≡C) group in alkyne groups[41].
  - In case of RS sample, new bands appear at 1710, 1585 cm^{-1} due to the stretching vibration of C=O [42]and a new band at 1212 due to (C-O) stretching, attributed possibly to phenol[41].

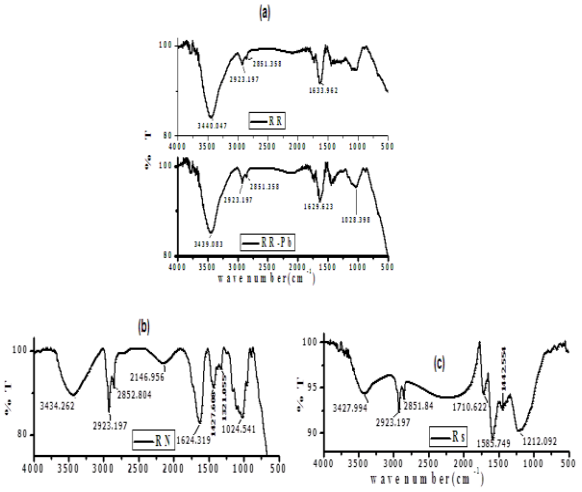

Figure1: FTIR spectra of (a) (RR and RR-Pb), (b) RN, (c) RS.

3.1.2 Scanning electron microscopy (SEM).

The morphology of the prepared orange peel derived bio-sorbents was done using SEM. The images were taken at different magnifications. These images explain how the activation methods affect the surface morphological properties of all samples .The SEM micrographs of RR, RN, and RS are shown in Figure (2, a-c). After treatment with sodium hydroxide, RN has more irregular and porous structure than that of RR, and therefore more specific surface area. This surface characteristic would result in the higher adsorption capacity. In case of RS the image revealed the presence of new porous structure on the surface and also higher surface area.

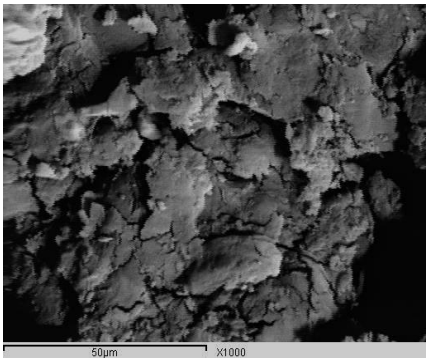

a

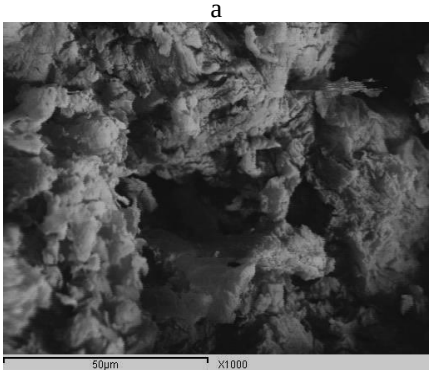

b

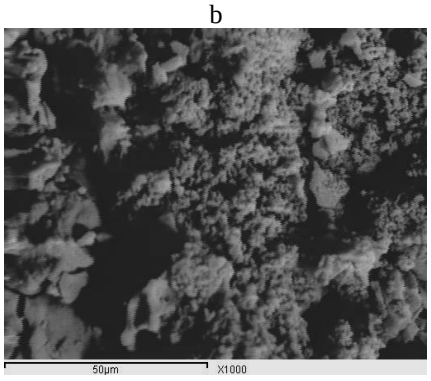

c

Figure 2: SEM micrographs: (a) RR; (b) (RN) and (c) (RS)

3.1.3 Energy Dispersive X-ray spectroscopy (EDX).

The results obtained from the EDX of RR, RN, RS and Pb (II) loaded RR sorbents are displayed in Fig.1S. The results indicate that, upon loading of Pb (II) the new content of lead ion appeared in case of RR sample at 2.342 ev showing a good percent of lead ion.

3.1.4 BET surface area analysis.

The N_2 adsorption–desorption isotherm was used to determine surface area using the Brunauer–Emmett–Teller (BET) equation. Gas adsorption measurements are widely used for the characterization of different types of porous solids such as (oxides, carbons, zeolites and organic polymers). The specific surface area (m^2/g) and porosity of the carbon are the most important textural properties that determine its capacity for adsorption. From Fig.S (a, b) we can

determine the surface area of the prepared RS sample by applying the BET equation. The surface area of the RS sample was determined using BET surface area. It was found that the surface area of RS is (162 m^2/g**.**

3.1.5. Surface pH, point of zero charge.

The pH_{PZC} and the pH of the solution which determine the charge on the surface will be present as mentioned in Table (1); the sample surface is positively charged and surface sitesare protonated at pH <pH_{PZC} and, but at pH >pH_{PZC} is negatively charged. This charge on the orange surface is one of the parameters which explain the adsorption characteristics[43]. In case of RR and RS samples their supernatant pH is slightly lower than their pH_{PZC}. The drastic decrease in pH_{PZC} of RS is due to the reaction of H_2SO_4 with carbonized orange peel as dehydrating agent. But in case of RN the supernatant pH is the same of pH_{PZC}. The plots to determine the pH of the point of zero charge (pH_{PZC}) are shown in Fig.3S.

Table 1: The obtained data of pH of supernatant and point of zero charge of the orange peel derived bio-sorbents.

Bio-sorbent	pH of supernatant	Point of zero charge
RR	6.23	6.029
RN	7.07	7.072
RS	3.95	3.30

RR=Raw orange peel, RN=NaOH modified orange peel, RS= H_2SO_4 modified orange peel

3.2. Biosorption of Pb (II).

3.2.1. Effect of initial pH on the adsorption of Pb (II).

The pH of the solution has a significant impact on the uptake of heavy metals, since it determines the surface charge of the adsorbent, the degree of ionization and speciation of the adsorbate. The effect of the pH solution on removal of Pb (II) on each of the prepared samples obtained was carried out in the pH ranges between 2 and 6.5. Studies above pH 6.5 was not performed, because in this case, lead ions are not found in their ionic states but present as a precipitated species $Pb(OH)_2$ [44] . The effect of pH value on Pb (II) ions adsorption capacity on different samples is shown in Figure 3. It can be noticed that, the adsorption capacity of Pb (II) ions increased with increasing pH of aqueous solution and reached maximum value at pH =(4.5-5). According to Low et al [45] little adsorption at lower pH could be ascribed to the hydrogen ions competing with metal ions for sorption sites. This means that at higher H^+ ion concentration, the adsorbent surface becomes more positively charged, thus, reducing the attraction between adsorbent and metal ions. In contrast as the pH increases, more negatively charged surface become available, thus, facilitating greater metal uptake[46]. At a higher pH, lead ions precipitated as their hydroxides which decreased the rate of adsorption and subsequently the percent removal of metal ions.

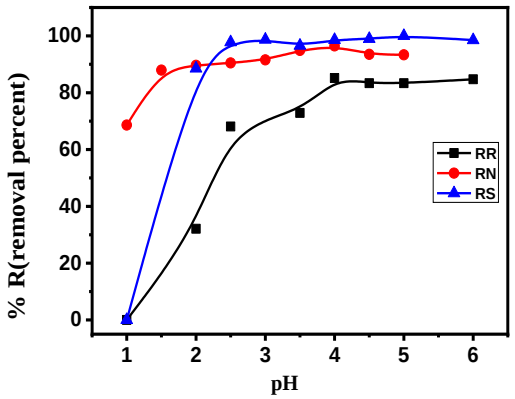

Figure 3: Effect of pH on adsorption of Pb (II) ion on RR, and RN, and RS.

3.2.2. The effect of initial concentrations.

The metal uptake depends mainly on the initial metal ion concentration. The effect of concentration and temperature is shown in Figure 4. It can be noticed that, the adsorption capacity of Pb (II) ions increases with increasing initial metal ion concentration. This is due to the increasing in the driving forces of the initial metal concentration which play very important role in overcoming all mass transfer resistances between the aqueous and solid phases[47]. Also the increasing in the adsorption capacity of Pb (II) ions is due to the availability of active sites for metal binding with the activated samples, by the time these active and exchange sites become more saturated with metal ions[48] .

The adsorption capacity of Pb (II) ions increases on activated samples in the following order RS>RN>RR. From this arrangement we can observe the effect of the activation on the adsorption capacity. On the other hand, temperature has a profound effect on heavy metal removal by using various adsorbents and the optimum temperature for better removal changes with the type of adsorbent and adsorbate. It is observed that, the adsorption capacity increases with increasing temperature in case of (RS) samples, but decrease in case of (RR, and RN) samples. This nature of samples will be explained from the thermodynamic studies.

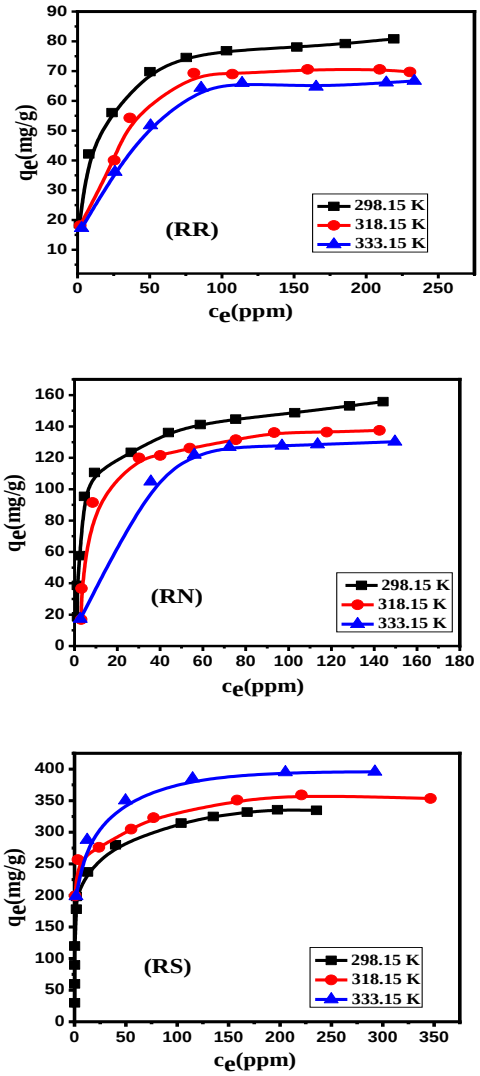

Figure 4: Adsorption isotherm of Pb(II) on different (a) RR, (b) RN, and (c) RS samples.

3.2.3. Effect of adsorbent dosage

In order to determine the appropriate adsorbent dose of activated carbon, the adsorbent dose of RR, and RN were varied from (0.01-0.25) gm. As shown in Figure (5), the removal of Pb (II) increases with increasing the adsorbent dose (but the adsorption capacity decreases). This may be attributed to that as the adsorbent dose increases, the available active sites for adsorption and surface area increase causing increasing in adsorption. The decreasing in adsorption density with increasing the adsorbent dose is mainly because of instauration of adsorption sites through the adsorption process[49, 50].

3.2.4. Effect of contact time.

Shaking time is an important factor in adsorption process of lead ions on activated carbon. The effect of contact time was studied to determine the maximum time that is required for reaching the equilibrium state.

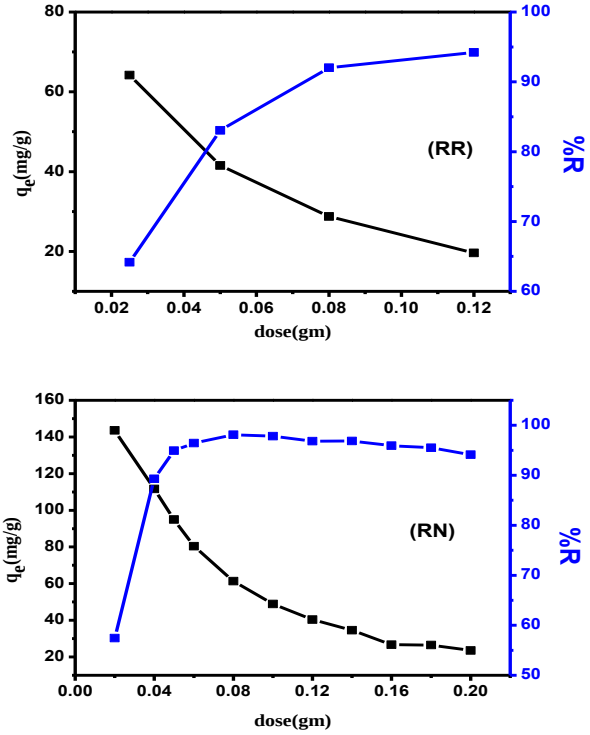

Figure 5: Effect of adsorbent dosage of (a) RR, and (b) RN samples for Pb (II) removal

The effect of contact time on adsorption was studied between 5 and 350 min. The results are presented in Fig.4S. The metal uptake increases with time and reached the equilibrium state at (100 min) in case of (RR, and RN) and at (150 min) in case of RS sample. After this equilibrium period, the amount of adsorbed of Pb (II) ions does not significantly change with time. From this figure we can notice that, the adsorption rate is very fast at first (50 min), may be due to an availability of large number of vacant (active) sites on the adsorbent at the initial stage, so that, there was an increase in concentration gradients between adsorbate in solution and adsorbate on adsorbent surface subsequently, increasing in Pb (II) ions sorption at the initial stages. As time increases, this concentration is reduced due to the accumulation of Pb (II) ions particles in the vacant sites leading to decrease in the adsorption rate and active sites become more saturated and the exchange sites become more full[48] .Therefore, 2 h is chosen as the optimum adsorption time for the experimental test to ensure that equilibrium is achieved.

3.2.5. Equilibrium adsorption isotherms studies.

Equilibrium study on adsorption provides information on the capacity of the adsorbent. An adsorption isotherm is characterized by certain constant values, which express the surface properties and affinity of the adsorbent and can also be used to compare the adsorptive capacities of the adsorbent for

different pollutants[51, 52].The several adsorption isotherm models like Langmuir, Frendulich, Temkin, and Redlich-peterson have been used to test the equilibrium kinetics data[53]. In our study, adsorption data were employed to two isotherm models, Freundlich and Langmuir models.

For Langmuir isotherm: Langmuir theory based on the assumption that adsorption is a type of chemical combination and the adsorbed layer is unimolecular

This model can be expressed in its linear formula as:

$$\frac{c_e}{q_e} = \frac{1}{bq} + \frac{c_e}{q} \qquad \textbf{(4)}$$

Where $\mathbf{C_e}$ is the equilibrium Pb (II) concentration (**mg/l**), $\mathbf{q_e}$ the amount of the Pb (II) adsorbed per unit weight of the adsorbent for monolayer capacity (**mg/g**) and b is the Langmuir equilibrium constant (**l/mg**). Both q_e and b can be determined from a linear plot of $\mathbf{Ce/q_e}$ versus **Ce** as shown in Figure (6). The favourable nature of adsorption can be evaluated by determination the dimensionless separation factor of equilibrium parameter R_L, which is expressed as:

$$R_L = \frac{1}{1+K_L C_O} \qquad \textbf{(5)}$$

Where C_o in this case is the highest initial solute concentration and K_L is Langmuir constant. The values of RL indicates the type of isotherm to be irreversible where (R_L=0), favorable (0< R_L<1), linear (R_L=1) or unfavorable (R_L>1)[54] .From the data that are tabulated in table (2), we noticed that the R_L is ranging from (0.008 to 0..051) which fall in the region of (0< R_L<1) indicating that the adsorption process of Pb (II) on the prepared activated samples in this study is favourable.

For Freundlich isotherm: it describes physical adsorption from and adsorption model stipulates that the ratio of solute adsorbed to the solute concentration is a function of the solution.

The Freundlich isotherm is often used for heterogeneous surface energy systems [14]. Its linear formula can be expressed as:

$$\log q_e = \log K_F + \frac{1}{n}\log C_e \qquad \textbf{(6)}$$

Where $\mathbf{K_F}$ **(l/mg)** is Freundlich constant and **n** is Freundlich exponent. These two parameters ($\mathbf{K_F}$ **and 1/n**) can be determined from intercept and slope from a linear plot of log qe versus log **Ce** as shown in the data that are graphed in Figure 7. K_F can be defined as the adsorption or distribution coefficient and represents the quantity of Pb (II) adsorbed onto activated samples for a unit equilibrium concentration (a measure of adsorption capacity, ($mg.g^{-1}$)[55] .1/n value is very important in determination of adsorption intensity or surface heterogeneity[56]. Higher the value of 1/n, the higher will be the affinity between the adsorbate and the adsorbent, and the heterogeneity of the adsorbent sites.

In this study the value of 1/n <1 indicating that Pb (II) is convenient to be adsorbed on the surface of activated samples at all temperatures[57]. In this study we can conclude that, the adsorption process obey the Langmuir adsorption model and this is very clearly from the value of correlation coefficients (R^2) in all cases of the prepared samples as shown in table (2) that is larger than that in Freundlich model, Where R^2 is ranging from (0.988) to (0.999) in case of Langmuir model and from (0.740 to 0.992) in Freundlich isotherm. Figures (6 and 7) and Table (2) explain the total results of adsorption isotherms.

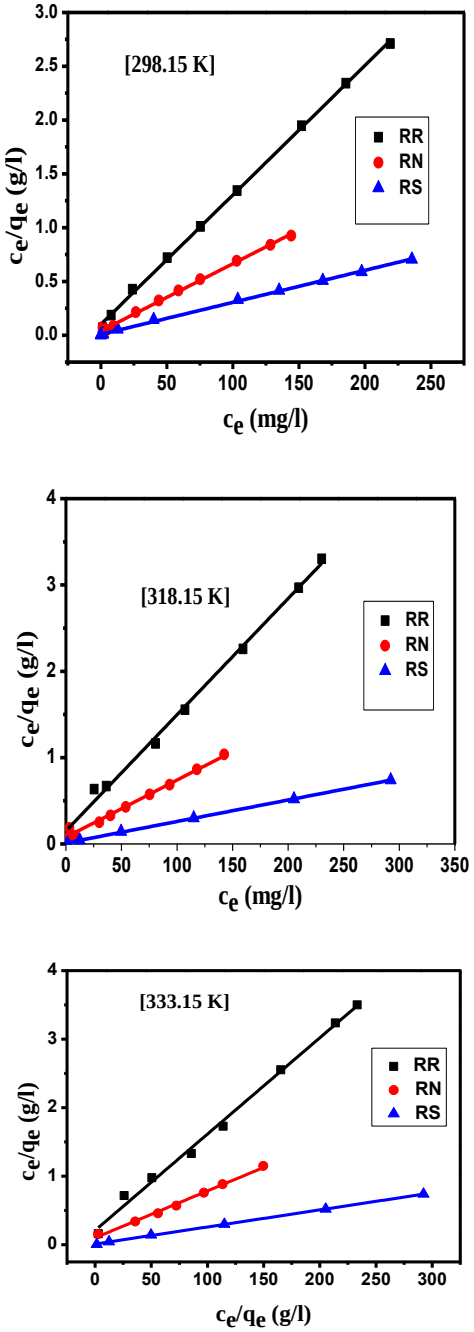

Figure 6: Adsorption isotherm Langmiur model for Pb (II) at different temperature for RR, RN, and RS.

Table 2: Langmuir and Freundlich isotherm constants for Pb (II) adsorption

	Temp	298.15 K				318.15 K				333.15 K			
Langmuir	biosorbent	q_{max} (mg/g)	b (L/mg)	R_L	R^2	q_{max} (mg/g)	b (L/mg)	R_L	R^2	q_{max} (mg/g)	b (L/mg)	R_L	R^2
	RR	83.06	0.119	0.027	0.999	74.29	0.089	0.036	0.995	71.17	0.067	0.047	0.995
	RN	159.74	0.162	0.020	0.998	150.83	0.086	0.039	0.988	146.19	0.067	0.051	0.994
	RS	353.36	0.083	0.021	0.999	366.3	0.113	0.012	0.999	404.86	0.166	0.008	0.999
Freundlich		K_f (mg/g)		1/n	R^2	K_f (mg/g)	1/n	R^2		K_f (mg/g)	1/n	R^2	
	RR	1.883		1.32051	0.92497	1.964	1.21156	0.9327		2.079	1.12395	0.94202	
	RN	1.374		1.89886	0.98756	1.390	1.84678	0.93904		1.381	1.82394	0.74059	
	RS	1.357		2.22503	0.99231	1.262	2.31041	0.91168		1.357	2.29729	0.96098	

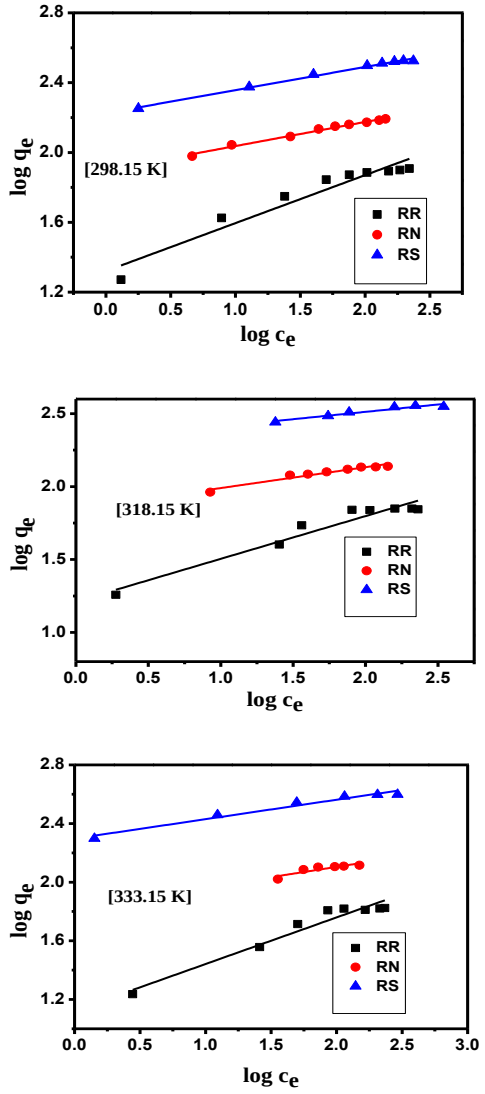

Figure 7: Adsorption isotherm Freundlich model for Pb (II) at different temperature for RR, RN, and RS.

3.3. Adsorption kinetics.

Adsorption kinetic study is important in determining the efficiency of adsorption. Kinetic models have been applied to study the experimental data and to determine the mechanism of adsorption and its potential rate-controlling step that include mass transfer and chemical reaction. Adsorption kinetics expressed as the solute removal rate that controls the residence time of the adsorbate in solid-solution interface. In the present work, the kinetic data obtained from batch studies has been determined by using the pseudo first-order model, pseudo second-order model, the intraparticle diffusion model, and Boyd model.

3.3.1. Pseudo first-order equation.

Lagergren proposed a pseudo-first-order kinetic model. This model was successfully applied to describe the kinetics of many adsorption systems[58] .This model can be expressed in its linear formula from the following equation[59] :

$$\log(q_e - q_t) = \log q_e - \frac{k_1}{2.303} t \qquad (7)$$

Where q_e (mg/g) and q_t **(mg/g)** are the amount of Pb (II) adsorbed at equilibrium and the amount of Pb (II) adsorbed at time t (min) respectively. K_1 and q_e were determined from the slope and intercept of linear plot of log $(q_e - q_t)$ versus t as shown in Figure (8.a).

3.3.2. Pseudo second-order equation.

The adsorption kinetics may also be described by a pseudo-second-order kinetic model[60, 61] :

$$\frac{t}{q_t} = \frac{1}{k_2 q_e^2} + \frac{1}{q_e} t \qquad (8)$$

Where, K_2 (g mg^{-1} min^{-1}) is the second order rate constant. Both K_2 and q_e can be obtained from the linear plot of t/qt against t as shown in Figure (8.b). Determination of the best model from these two kinetics models was achieved by the comparison of the correlation coefficients of both models as shown in Table (3) for the selected activated carbon sample.

By analysis the data obtained in Table (3), we can estimate that, pseudo-second order model is the best model that can successfully describe the adsorption kinetics of this system, where R^2 in case of pseudo-second order model **(0.999)** is higher than in case of pseudo-first order model **(ranging between 0.726-0.986)** giving high linearity nature. Also the q_2 in case of pseudo-second order model is very close to the experimental value than in case of pseudo-first order model.

3.3.3. Intra-Particle Diffusion.

In adsorption process, it is important to determine the rate determining step (slowest step).

Generally, in solid-liquid adsorption system, adsorption process is usually characterized by either external mass transfer or intraparticle diffusion or both. Intra-particle diffusion can be expressed from the following equation[62] :

$$q_t = k_{int}\, t^{0.5} + c \qquad (9)$$

Where q_t, k_{int} and C, refers to the amount of Pb (II) adsorbed in mg/g at time, t; intra-particle diffusion rate constant and constant respectively (where C is the intercept), which can be determined from plotting of q_t versus $t^{0.5}$.this equation also called Weber-Morris. They found that in many adsorption cases, solute uptake varies almost proportionally with $t^{0.5}$ rather than with the contact time t[63].

According to Eq. (9), a plot of q_t.vs.$t^{0.5}$ should be a straight line with a slope k_{int} when the intraparticle diffusion is a rate-limiting step. For Weber-Morris model, it is essential for the q_t.*vs.* $t^{0.5}$ plot to go through the origin if the intraparticle diffusion is the slow rate-limiting step. However, it is not always the case at which intraparticle diffusion is the slow rate-limiting step and adsorption kinetics may be controlled by film diffusion and intraparticle diffusion simultaneously. Thus, the slope is not equal to zero.

3.3.4. Boyd Model.

Due to the double nature of intra-particle diffusion (both film and pore diffusion), and in order to determine the ***actual*** rate-controlling step (either intarparticle diffusion or film diffusion), the kinetic data were further analyzed by using Boyd model. Boyd kinetic equation[64] is represented as:

$$F(t) = 1 - \frac{6}{\pi^2}\sum_{n=1}^{\infty}\frac{1}{n^2}\exp(-n^2 Bt) \qquad (10)$$

Where F is the fraction of solute adsorbed at any time (t), and B (t) is mathematical function of F, where n is an integer that defines the infinite series solution and F is the fractional attainment of equilibrium at time t which is determined by the expression:

$$F = \frac{q_t}{q_q} \qquad (11)$$

Where, q_e is the amount of Pb (II) adsorbed at equilibrium (mg/g) and q_t represents the amount of Pb (II) adsorbed at any time t (min). Reichenberg [65] managed to obtain the following approximations:

For F values > 0.85;

B (t) = -0.4977-ln (1-F) **(12)** For F values < 0.85;

$$B(t) \sqrt{\pi}\sqrt{\pi - (\frac{\pi^2 F(t)}{3})} \qquad (13)$$

From Figure (8.c) we can observe that, the linear plots don't pass through the origin so the rate determining step isn't controlled by intarparticle diffusion, but also affected by film diffusion. In case of Figure (8 d) (Boyed model), also the linear plots don't pass through the origin, so that the rate the rate determining step in case of adsorption of Pb (II) is film diffusion step.

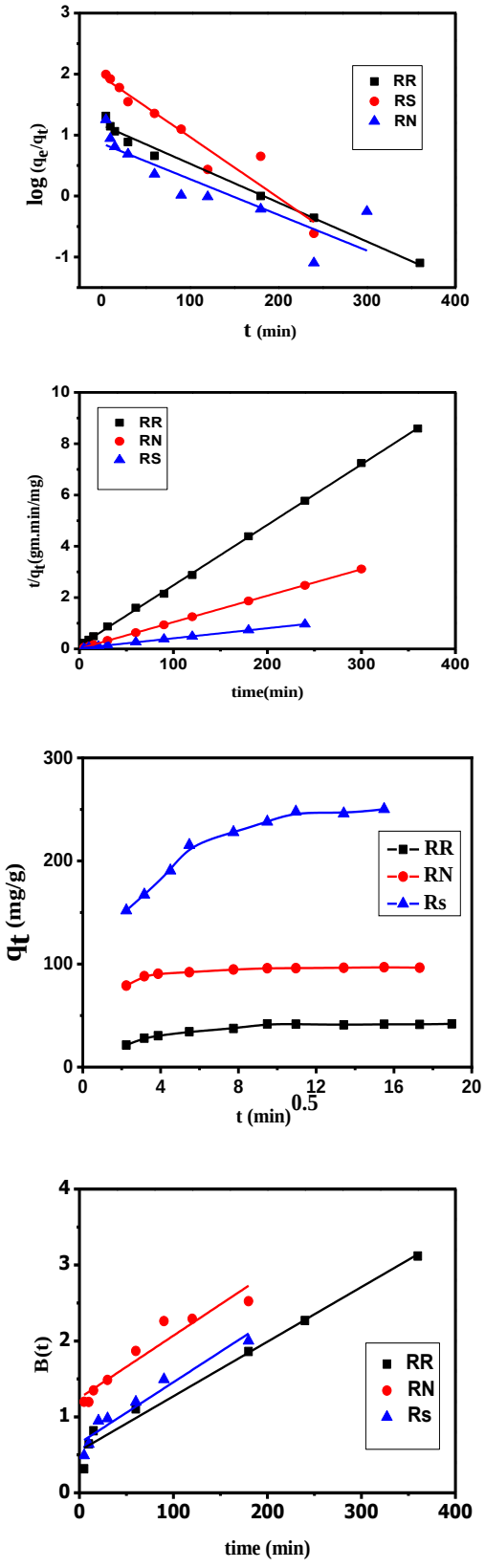

Figure 8: kinetic models for adsorption of Pb (II): - (a) Pseudo-first order, (b) Pseudo-second order, (c) Intra particle diffusion, and (d) boyed model on activated sample.

Table 3: Kinetic parameters for the adsorption of for Pb (II) adsorption

biosorbent samples		RR	RN	RS
	$q_{e,exp}$(mg/g)	41.92	96.44	250.26
First-order kinetic equation	**q_1 (mg/g)**	14.77	7.313	92.036
	k_1 (1/min)×10^{-3}	14.69	13.49	22.92
	R_1^2	0.98651	0.72598	0.9201
Second-order kinetic equation	**q_2 (mg/g)**	42.43	96.99	255.10
	k_2 [g/(mg min)]x10^{-4}	5.555	8.645	7.068
	R_2^2	0.99969	0.99998	0.99966
Intraparticle diffusion equation	**k_{int} [mg/(g $min^{1/2}$)]**	1.53542	0.97755	5.88438
	C	25.21297	86.30734	182.7448
	R_{int}^2	0.97314	0.91084	0.99742
Boyd equation	**Intercept**	0.55394	1.24795	0.65434
	R^2	0.97752	0.90533	0.92427

3.4. Thermodynamic studies

The adsorption nature of Pb (II) on the prepared activated samples was predicted by estimating the thermodynamic parameters. The Langmuir constant ***b*** changing with temperature can be used to calculate the thermodynamic parameters enthalpy (ΔH·), free energy change (ΔG°) and entropy change (ΔS°). Change in the Gibbs free energy (ΔG°) indicates the degree of the spontaneity of the process. It can be calculated from the following equation:

$\Delta G^o = -RT\ln b$. **(14)**

Where ***T*** is the temperature in (***K***), ***R*** is the universal gas constant ***(8.314 × 10−3 kJ/mol K)*** and ***b*** is Langmuir constants ***(l/mole).*** Change in enthalpy ***(ΔH°)*** and change in entropy ***(ΔS°)*** can be estimated from the following equations that called Van't Hoff equation[66] :

$$\ln b = \frac{-\Delta H^o}{RT} + \frac{\Delta S^O}{R} \quad (15)$$

(ΔH°) and ***(ΔSo)*** can be determined from linear plot of ***ln b*** versus ***1/T*** from slope and intercept respectively. Where, the slope and intercept of Van't Hoff plot are equal to $\left(\frac{-\Delta H^0}{R}\right)$ and $\left(\frac{\Delta S^O}{R}\right)$ respectively. The data of ***ΔG°,*** ***ΔH°*** and ***ΔS°*** are tabulated in table (4.10).

Figure (9) and Table (4) conclude all thermodynamic parameters. ΔH° has a positive value in RS sample indicating an endothermic nature of adsorption process where the Pb (II) uptake increases with increasing temperature, but in case of (RR, and RN) ΔH° has a negative value indicating an exothermic nature of adsorption process where the Pb (II) uptake decreases with increasing temperature. From the data that are mentioned in Table (4), all samples have a negative ΔG° value confirming that, this process is spontaneous and ΔG° decreases with increasing temperature of the solution. Positive value of ΔS° that was observed in all samples proves the increasing in randomness at adsorbent-adsorbate interface during the adsorption process with high affinity of these activated samples for Pb (II) with some changes in the structure in the adsorbate-adsorbent system for Pb (II) adsorption[67].

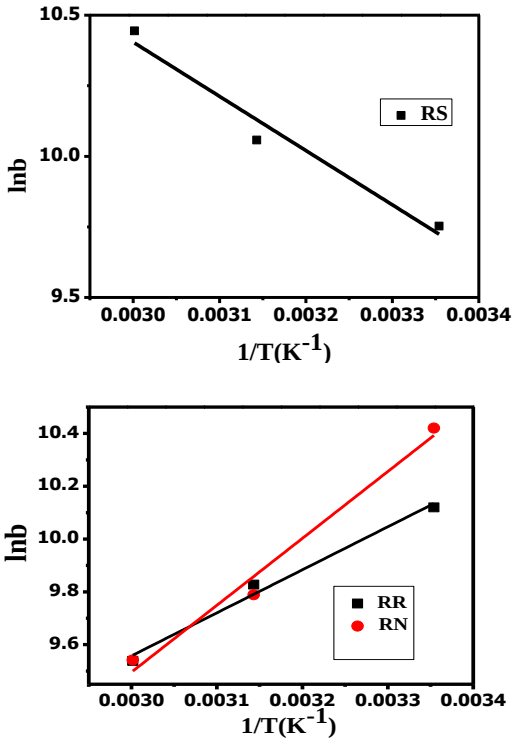

Figure 9: Van't Hoff isotherm for adsorption of Pb (II) on RS, RR, and RN sample.

Table 4: Thermodynamic parameters for the adsorption of Pb (II) on RS, RR, and RN.

Sample	ΔS^0(J/mole K)	ΔH^0(kJ/mole)	ΔG^0(kJ/mole)		
			298.15	318.15	333.15
RS	134.44	15.978	-23.53	-26.186	-28.495
RR	38.82	-13.548	-24.41	-25.585	-26.023
RN	15.76	-21.061	-25.14	-25.48	-26.032

3.5. Ionic strength effect.

Ionic strength effects on metal ion adsorption have been studied by changing either solute activity or diffuse electrical double layer thickness. Ionic strength also affects the adsorption of metal ions through changing the aqueous metal chemistry and the structure of the electric double layer surrounding the adsorbent surface[68]. This effect was studied at 10 mg/l of Pb (II) on (RN, RS, and RR) samples and varying the NaCl solution concentration between (0.001-0.15) M at normal pH (without any adjustment of pH) to avoid any interfering of buffer solution during study this effect. In Fig.5 S , the metal removal increases from (0.001-0.05) M NaCl solution, by increasing of NaCl solution concentration, the metal removal decreases. The increasing in removal percentage may be due to the compression of the activated samples electrostatic double layer when ionic strength of the solution increased according to the electrostatic double layer (EDL) theory[69]. Hence, adsorption of metal ions increased. However, the decreasing in removal percentage at ionic strength > 0.05 could be attributed to the competitive effect between pb (II) ions and cations from the salt (Na^+) for the sites available to the sorption process[70, 71] .

3.6. Foreign ions Effect.

The removal of heavy metals is strongly affected by natural water matrix (anions and cations) which can be present in the water sources. To study this effect, adsorption of Pb (II) was performed in the presence of different ions which are available in drinking water such as, fluoride, oxalate, and acetate, Ca^{2+}, KH_4^+ and Mg^{2+}. Their effect was tabulated in table (5). The concentration of foreign ions in case of (RN) is 200 mg/l and 100 mg/l in case of (RR and RS).We can notice that the removal of lead is not affected badly by the foreign ions. This proves the efficiency of these adsorbents in removal of lead ions from water without any problems that can be present due to the presence of water matrix.

Table 5: Effect of foreign ions on the removal of 10 mg/l Pb (II) using RN, RR, &RS.

Foreign ions	% R of Pb (II)		
	RN	RR	RS
Ca^{2+}	8.1	77.43	91.23
Mg^{2+}	---	72.97	80.77
Na^+	93.1	94.73	99.65
K^+	93.6	---	---
NH_4^+	---	95.63	100.1
F^-	91.7	95.73	100
Cl^-	94.9	99.06	95.31
$Oxalate^-$	93.7	97.3	99.68
$Acetate^-$	95	97.6	100.47

3.7. Analytical applications using RR, RN and RS samples.

The applicability of the (RR) for removal of Pb (II) from different water samples such as distilled water, tap water, and Alexandria sea water was studied. 20mg/l of Pb (II) was spiked in PVC flasks containing 25 ml the mentioned water samples, and 0.025 gm of the adsorbents. The filtrate was analyzed. The data that were obtained is shown in Table (6).

From the data in Table (6), we can observe that, the prepared bio-sorbents can remove the lead metal ions in the presence of the different matrix in water samples with high efficiency.

Table 6: Recovery of Pb (II) from different water samples using the prepared orange peel derived bio-sorbent Pb (II): Sorbents :(RR, RN, and RS) samples at pH: 5; Temp.: 25 ℃ (n=3).

Water Sample (Location)	Pb (II) Found (mg/l)	Recovery (R, %)		
		RR	RN	RS
Bi-distilled water	0.5	85	93.33	99.5
Tap water	1.01	81.97	96.22	98.05
Sea water (Alexandria)	1.30	87	93.8	97.04
Sea water (Damietta)	1.28	87.2	94	96.50

Pb (II) Found in (mg/l):-is the actual concentration of lead calculated in the studied water samples

3.9. Desorption Studies.

The commercial efficiency of the activated samples is measured by their ability to be desorbed from the loaded contaminants.

In order to find how the prepared bio-sorbents can be reused again or not, desorption studied were performed using different concentrations of HCl. To study this effect, the (RR, RN) samples were loaded with Pb (II) then filtrated. The filtrate was analyzed. As shown in Table (7):-

In case of RN sample the maximum desorption was obtained at (0.4 M) HCl by 97.74% percentage

In case of RR sample, the maximum desorption was obtained at (0.3 M) HCl by 101.14%.

Table 7: Desorption effect on RN and RR samples.

HCL Conc.	% Desorption	
	RN	RR
0.1M	83.32	84.73
0.2M	87.66	86.07
0.3M	89.92	101.14
0.4M	97.74	96.37

4. Comparison of the proposed adsorbents with other cited adsorbents.

A comparison between the performance of the present adsorbents and other adsorbents previously reported in the literature is presented in Table 8. When comparing different adsorbents for the separation of lead (II), the sorption capacity and the type of sample matrices on which the separation is performed should

be taken into consideration. As shown in Table 8, the present adsorbents have relatively high capacities for the recovery of Pb (II) compared to other adsorbents [72-76].

Table 8: Comparison of maximum sorption capacity of Pb (II) by proposed orange peel derived bio-sorbents with previously published adsorbents.

Adsorbent	q_e (adsorption capacity) mg/g	temperature	References
RR	80.83	25	Present study
RN	155.8	25	Present study
RS	334.6	25	Present study
H2SO4-treated CNS	8.73	30	[72]
Plum kernel	1.3	22	[73]
Peanut shell	7.13	30	[74]
Soya bean seed	0.72	28	[75]
Mushroom biomass	3.89	room	[76]

5. Conclusion

From this study we can confirm that orange peel as a very cheap biosorbent can be considered as an effective adsorbent in the removal of lead ions from water. Sodium hydroxide (NaOH) modified orange peel (RN) and sulfuric acid activated orange peel (RS) exhibit highly adsorption capacity of lead ions per gram of each prepared samples where uptake of lead ion was 80.83mg/g, 155.8mg/g, 334.6mg/g for RR, RN, RS samples respectively and this is a very high uptake for metal ion removal in comparison with other prepared samples as shown in Table 8. The chosen pH for maximum lead ion uptake was pH 5 without any precipitation of lead because it was observed that above this pH the adsorption of lead was not correct because it precipitates at higher pH. The adsorption process fitted more to Langmuir isotherm and obeys pseudo second order from kinetic study. The prepared samples can be easily applied in different source of water because we observed that they can remove lead ions from water matrices with highly percent. Also, they can be reused as shown from desorption study which showed that the prepared samples can be easily reused after desorption process.

References

1. Ali, I. and V. Gupta, Advances in water treatment by adsorption technology. Nature Protocols, 2007. **1**(6): p. 2661-2667.
2. Gupta, V., et al., Low-cost adsorbents: growing approach to wastewater treatment—a review. Critical Reviews in Environmental Science and Technology, 2009. **39**(10): p. 783-842.
3. Ayyappan, R., et al., Removal of Pb (II) from aqueous solution using carbon derived from agricultural wastes. Process Biochemistry, 2005. **40**(3): p. 1293-1299.
4. Mahurpawar, M., Effects of heavy metals on human health. International Journal of Research-Granthaalayah, 2015. **3**(9SE): p. 1-7.
5. Gupta, V.K., M. Gupta, and S. Sharma, Process development for the removal of lead and chromium from aqueous solutions using red mud—an aluminium industry waste. Water Research, 2001. **35**(5): p. 1125-1134.
6. Abdel-Shafy, H.I. and R.O. Aly, Wastewater management in Egypt, in Wastewater Reuse–Risk Assessment, Decision-Making and Environmental Security. 2007, Springer. p. 375-382.
7. Priority List of Hazardous Substances. . Available from: http://www.atsdr.cdc.gov/spl/.
8. Mallikarjuna, N. and A. Venkataraman, Adsorption of Pb^{2+} ions on nanosized γ-Fe_2O_3: formation of surface ternary complexes on ligand complexation. Talanta, 2003. **60**(1): p. 139-147.
9. Takeno, N., Atlas of Eh-pH diagrams. Geological survey of Japan open file report, 2005(419).
10. Low, K., C. Lee, and S. Liew, Sorption of cadmium and lead from aqueous solutions by spent grain. Process Biochemistry, 2000. **36**(1): p. 59-64.
11. Environmental Protection Agency (US EPA) National Primary drinking Water Regulations 2011. Available from: http://www.epa.gov/safewater/mcl.html.
12. Kausar, A., et al., A green approach for the removal of Sr (II) from aqueous media: kinetics, isotherms and thermodynamic studies. Journal of Molecular Liquids, 2018. **257**: p. 164-172.
13. Fakhre, N.A. and B.M. Ibrahim, The use of new chemically modified cellulose for heavy metal ion adsorption. Journal of hazardous materials, 2018. **343**: p. 324-331.
14. Örnek, A., M. Özacar, and İ.A. Şengil, Adsorption of lead onto formaldehyde or sulphuric acid treated acorn waste: equilibrium and kinetic studies. Biochemical Engineering Journal, 2007. **37**(2): p. 192-200.
15. Akl, M.A., et al., Application of crosslinked ionic poly (vinyl alcohol) nanogel as adsorbents for

water treatment. Journal of dispersion science and technology, 2013. **34**(10): p. 1399-1408.
16. Shoueir, K.R., et al., New core@ shell nanogel based 2-acrylamido-2-methyl-1-propane sulfonic acid for preconcentration of Pb (II) from various water samples. Applied Water Science, 2017. **7**(7): p. 3729-3740.
17. Mostafa, A.G., et al., Selective separation of Cu (II) from a single metal ion solution by using O-amino thiophenol-modified flax fiber. Egyptian Journal of Chemistry, 2021. **64**(4): p. 2-3.
18. Saleh, M.O., M.A. Hashem, and M. Akl, Removal of Hg (II) metal ions from environmenta water samples using chemically modified natural sawdust. Egyptian Journal of Chemistry, 2021. **64**(2): p. 1027-1034.
19. Matlock, M.M., B.S. Howerton, and D.A. Atwood, Chemical precipitation of lead from lead battery recycling plant wastewater. Industrial & engineering chemistry research, 2002. **41**(6): p. 1579-1582.
20. Kenawy, I., et al., Determination by AAS of some trace heavy metal ions in some natural and biological samples after their preconcentration using newly chemically modified chloromethylated polystyrene-PAN ion-exchanger. Analytical sciences, 2000. **16**(5): p. 493-500.
21. Hafez, M., et al., Preconcentration and separation of total mercury in environmental samples using chemically modified chloromethylated polystyrene-PAN (ion-exchanger) and its determination by cold vapour atomic absorption spectrometry. Talanta, 2001. **53**(4): p. 749-760.
22. Dąbrowski, A., et al., Selective removal of the heavy metal ions from waters and industrial wastewaters by ion-exchange method. Chemosphere, 2004. **56**(2): p. 91-106.
23. Páez-Hernández, M.E., et al., Mercury ions removal from aqueous solution using an activated composite membrane. Environmental science & technology, 2005. **39**(19): p. 7667-7670.
24. Monier, M., M. Akl, and W.M. Ali, Modification and characterization of cellulose cotton fibers for fast extraction of some precious metal ions. International journal of biological macromolecules, 2014. **66**: p. 125-134.
25. Lasheen, M.R., N.S. Ammar, and H.S. Ibrahim, Adsorption/desorption of Cd (II), Cu (II) and Pb (II) using chemically modified orange peel: Equilibrium and kinetic studies. Solid State Sciences, 2012. **14**(2): p. 202-210.
26. Tsai, W., et al., Utilization of agricultural waste corn cob for the preparation of carbon adsorbent. Journal of Environmental Science and Health, Part B, 2001. **36**(5): p. 677-686.
27. Feng, N., et al., Biosorption of heavy metals from aqueous solutions by chemically modified orange peel. Journal of hazardous materials, 2011. **185**(1): p. 49-54.
28. Juang, R.-S., F.-C. Wu, and R.-L. Tseng, Characterization and use of activated carbons prepared from bagasses for liquid-phase adsorption. Colloids and Surfaces A: Physicochemical and Engineering Aspects, 2002. **201**(1): p. 191-199.
29. Toles, C.A. and W.E. Marshall, Copper ion removal by almond shell carbons and commercial carbons: batch and column studies. Separation science and technology, 2002. **37**(10): p. 2369-2383.
30. El-Shafey, E., Sorption of Cd (II) and Se (IV) from aqueous solution using modified rice husk. Journal of hazardous materials, 2007. **147**(1): p. 546-555.
31. Martín-Lara, M.Á., et al., Modification of the sorptive characteristics of sugarcane bagasse for removing lead from aqueous solutions. Desalination, 2010. **256**(1): p. 58-63.
32. Adebayo, G., A. Mohammed, and S. Sokoya, Biosorption of Fe (II) and Cd (II) ions from aqueous solution using a low cost adsorbent from orange peels. Journal of Applied Sciences and Environmental Management, 2016. **20**(3): p. 702-714.
33. Kamsonlian, S., et al., Characterization of banana and orange peels: biosorption mechanism. International Journal of Science Technology & Management, 2011. **2**(4): p. 1-7.
34. Moreno-Piraján, J.C. and L. Giraldo, Heavy metal ions adsorption from wastewater using activated carbon from orange peel. E-journal of chemistry, 2012. **9**(2): p. 926-937.
35. Tejada-Tovar, C., A. Gonzalez-Delgado, and A. Villabona-Ortiz, Removal of Cr (VI) from aqueous solution using orange peel-based biosorbents. Indian Journal of Science and Technology, 2018. **11**(13): p. 1-13.
36. Faisal, M.L., S.Z. Al-Najjar, and Z.T. Al-Sharify, Modified Orange Peel as Sorbent in Removing of Heavy Metals from Aqueous Solution. 2020.
37. Villabona-Ortiz, Á., et al., Removal of Cr (VI) ions from aqueous solution using orange peel residual biomass: Thermodynamic and sorption-desorption study. Desalination Water Treat, 2020. **203**: p. 309-314.
38. Feng, N.-C., X.-Y. Guo, and S. Liang, Enhanced Cu (II) adsorption by orange peel modified with sodium hydroxide. Transactions of nonferrous metals society of china, 2010. **20**: p. s146-s152.
39. Smičiklas, I., et al., The point of zero charge and sorption of cadmium (II) and strontium (II) ions on synthetic hydroxyapatite. Separation and

Purification Technology, 2000. **18**(3): p. 185-194.
40. Gerçel, Ö., et al., Preparation of activated carbon from a renewable bio-plant of Euphorbia rigida by H2SO4 activation and its adsorption behavior in aqueous solutions. Applied surface science, 2007. **253**(11): p. 4843-4852.
41. Yang, T. and A.C. Lua, Textural and chemical properties of zinc chloride activated carbons prepared from pistachio-nut shells. Materials chemistry and physics, 2006. **100**(2): p. 438-444.
42. Biniak, S., et al., The characterization of activated carbons with oxygen and nitrogen surface groups. Carbon, 1997. **35**(12): p. 1799-1810.
43. Nasiruddin Khan, M. and A. Sarwar, Determination of points of zero charge of natural and treated adsorbents. Surface Review and Letters, 2007. **14**(03): p. 461-469.
44. Giraldo-Gutiérrez, L. and J.C. Moreno-Piraján, Pb (II) and Cr (VI) adsorption from aqueous solution on activated carbons obtained from sugar cane husk and sawdust. Journal of Analytical and Applied Pyrolysis, 2008. **81**(2): p. 278-284.
45. Low, K., C. Lee, and K. Lee, Sorption of copper by dye-treated oil-palm fibres. Bioresource technology, 1993. **44**(2): p. 109-112.
46. Chang, J.-S., R. Law, and C.-C. Chang, Biosorption of lead, copper and cadmium by biomass of Pseudomonas aeruginosa PU21. Water Research, 1997. **31**(7): p. 1651-1658.
47. Hema, M. and K. Srinivasan, Uptake of toxic metals from wastewater by activated carbon from agro industrial by-product. Indian Journal of Engineering & Materials Sciences, 2010. **17**(5): p. 373-381.
48. Lehmann, R. and R. Harter, Assessment of copper-soil bond strength by desorption kinetics. Soil Science Society of America Journal, 1984. **48**(4): p. 769-772.
49. Shukla, A., et al., The role of sawdust in the removal of unwanted materials from water. Journal of Hazardous Materials, 2002. **95**(1): p. 137-152.
50. Yu, L.J., et al., Adsorption of chromium from aqueous solutions by maple sawdust. Journal of Hazardous Materials, 2003. **100**(1): p. 53-63.
51. Dash, S.N. and C.V.R. Murthy, Preparation of Carbonaceous Heavy Metal Adsorbent from Shorea Robusta Leaf Litter Using Phosphoric Acid Impregnation. International Journal of Environmental Sciences, 2010. **1**(3): p. 296-313.
52. Uddin, M., M. Islam, and M. Abedin, Adsorption of phenol from aqueous solution by water hyacinth ash. ARPN Journal of Engineering and Applied Sciences, 2007. **2**(2): p. 11-17.
53. Zeldowitsch, J., Adsorption site energy distribution. Acta Physicochim, URSS, 1934. **1**: p. 961-973.
54. Hamdaoui, O., Batch study of liquid-phase adsorption of methylene blue using cedar sawdust and crushed brick. Journal of hazardous materials, 2006. **135**(1): p. 264-273.
55. Amin, N.K., Removal of reactive dye from aqueous solutions by adsorption onto activated carbons prepared from sugarcane bagasse pith. Desalination, 2008. **223**(1): p. 152-161.
56. Haghseresht, F. and G. Lu, Adsorption characteristics of phenolic compounds onto coal-reject-derived adsorbents. Energy & Fuels, 1998. **12**(6): p. 1100-1107.
57. Khare, P., Treatment of Phenolic Water Using Adsorption. Unpublished Msc. Thesis], National Institute of Technology, Rourkela, 2011.
58. Gottipati, R., Preparation and Characterization of Microporous Activated Carbon from Biomass and its Application in the Removal of Chromium (VI) from Aqueous Phase, 2012.
59. Yuh-Shan, H., Citation review of Lagergren kinetic rate equation on adsorption reactions. Scientometrics, 2004. **59**(1): p. 171-177.
60. Ho, Y.-S., Review of second-order models for adsorption systems. Journal of hazardous materials, 2006. **136**(3): p. 681-689.
61. Ho, Y.-S., Second-order kinetic model for the sorption of cadmium onto tree fern: a comparison of linear and non-linear methods. Water research, 2006. **40**(1): p. 119-125.
62. Srivastava, V.C., et al., Adsorptive removal of phenol by bagasse fly ash and activated carbon: equilibrium, kinetics and thermodynamics. Colloids and Surfaces A: Physicochemical and Engineering Aspects, 2006. **272**(1): p. 89-104.
63. Alkan, M., Ö. Demirbaş, and M. Doğan, Adsorption kinetics and thermodynamics of an anionic dye onto sepiolite. Microporous and Mesoporous Materials, 2007. **101**(3): p. 388-396.
64. Boyd, G., A. Adamson, and L. Myers Jr, The exchange adsorption of ions from aqueous solutions by organic zeolites. II. Kinetics1. Journal of the American Chemical Society, 1947. **69**(11): p. 2836-2848.
65. Reichenberg, D., Properties of ion-exchange resins in relation to their structure. III. Kinetics of exchange. Journal of the American Chemical Society, 1953. **75**(3): p. 589-597.
66. Do Duong, D., Adsorption analysis: equilibria and kinetics. Vol. 2. 1998: Imperial College Press.
67. Önal, Y., et al., Adsorption kinetics of malachite green onto activated carbon prepared from Tunçbilek lignite. Journal of hazardous materials, 2006. **128**(2): p. 150-157.

68. Yang, S., et al., Adsorption of Ni (II) on oxidized multi-walled carbon nanotubes: effect of contact time, pH, foreign ions and PAA. Journal of hazardous materials, 2009. **166**(1): p. 109-116.
69. Brunauer, S., P.H. Emmett, and E. Teller, Adsorption of gases in multimolecular layers. Journal of the American Chemical Society, 1938. **60**(2): p. 309-319.
70. Goertzen, S.L., et al., Standardization of the Boehm titration. Part I. CO_2 expulsion and endpoint determination. Carbon, 2010. **48**(4): p. 1252-1261.
71. Boehm, H., Chemical Identification of Surface Groups. Advances in catalysis, 1966. **16**: p. 179.
72. Nuithitikul, K., R. Phromrak, and W. Saengngoen, Utilization of chemically treated cashew-nut shell as potential adsorbent for removal of Pb (II) ions from aqueous solution. Scientific reports, 2020. **10**(1): p. 1-14.
73. Pap, S., et al., Synthesis of highly-efficient functionalized biochars from fruit industry waste biomass for the removal of chromium and lead. Journal of Molecular Liquids, 2018. **268**: p. 315-325.
74. OuYang, X.-K., L.-P. Yang, and Z.-S. Wen, Adsorption of Pb (II) from solution using peanut shell as biosorbent in the presence of amino acid and sodium chloride. BioResources, 2014. **9**(2): p. 2446-2458.
75. Gaur, N., et al., Adsorptive removal of lead and arsenic from aqueous solution using soya bean as a novel biosorbent: equilibrium isotherm and thermal stability studies. Applied Water Science, 2018. **8**(4): p. 1-12.
76. Kariuki, Z., J. Kiptoo, and D. Onyancha, Biosorption studies of lead and copper using rogers mushroom biomass 'Lepiota hystrix'. South african journal of chemical engineering, 2017. **23**(1): p. 62-70.